Journal of Information Systems Engineering and Management
2025, 10(21s)
e-ISSN: 2468-4376
https://www.jisem-journal.com/

Research Article

ROISegNet: A Region-Focused Deep Learning Framework for Precision-Driven Medical Image Segmentation

[1.] Preethi Veerlapalli, [2.] Dr. Sushama Rani Dutta

[1.] *Research Scholar, Department of Computer Science and Engineering, Koneru Lakshmaiah Education Foundation, Hyderabad-500075, Telangana, India. Email: preethireddyveerlapalli@gmail.com*

[2.] *Associate Professor, Department of Computer Science and Engineering, Koneru Lakshmaiah Education Foundation, Hyderabad-500075, Telangana, India. Email: sushamarani.dutta@klh.edu.in*

ARTICLE INFO

Received: 22 Dec 2024

Revised: 31 Jan 2025

Accepted: 15 Feb 2025

ABSTRACT

Breast cancer is still one of the leading causes of death in women globally. Breast thermography is a non-invasive imaging procedure that can be used as an early screening device to identify temperature irregularities that suggest breast malignancies can develop. Early diagnosis is key to achieving better treatment and survival outcomes. Automated methods for breast cancer detection have drawn much attention due to the proliferation of artificial intelligence (AI) and deep learning (DL). This paper presents a new deep learning model, ROISegNet, that enables accurate segmentation of the region of interest (ROI) from breast thermography images. Our method utilizes semantic segmentation approaches using an atrous convolution-based deep learning architecture that effectively extracts the area of interest (ROI) where the abnormality is present in the human body, which potentially helps in early diagnosis. ROISegNet employs an advanced decoder module in addition to Intelligent Segmentation of Breast ROI (ISBROI), thereby achieving high segmentation accuracy. Evaluation on a benchmark dataset called DMR-IR shows that compared to other state-of-the-art backbones networks like Atrous Convolution, VGG19, ResNet50, and InceptionV3, the model's peak accuracy is 98 63%.

Keywords: Deep Learning, Machine Learning, Breast Cancer, Atrous Convolution, ROISegNet, CSSA, Thermography.

INTRODUCTION

Breast cancer is more common than any other malignancy in women worldwide and is the cause of approximately 15% of cancer-related deaths in females. Imaging techniques, vascular system, physical examinations, and self-examinations support early detection. However, a biopsy is the gold standard for determining with certainty the presence of breast cancer. This is the cheapest and most reliable of the three tests; therefore, mammography is the preferred screening method. However, in cases with dense breast tissue, where most tumors < 2 mm are missed, it has limited effectiveness. And exposure to ionizing radiation is a worry, especially for younger women. Given these challenges, thermography has become a promising alternative for screening for breast cancer. A non-invasive instruction called thermal imaging, or thermography, allows the assessment of breast tissue temperature variation based on infrared (IR) thermal imaging without radiation exposure. This method may be helpful for younger women and those with large breasts, as no compression and radiation exposures will occur. The basic mechanism at the root of breast thermography is detecting infrared radiation from breast tissue, whereby abnormal heat patterns can indicate underlying neoplasia. Though mammographies are effective, they are patient-unfriendly and less effective for patients with denser breast tissues.

Despite some advantages, precisely segmenting breast regions in thermograms is still challenging. Manual approaches for breast tissue segmentation are tedious, and automated segmentation approaches are complex because of the irregular shapes of breast tissues and undefined borders. Several traditional machine learning (ML) techniques have been applied for breast cancer detection using thermography. In contrast, deep learning (DL) methods have shown a high performance for feature extraction and image classification. Although Convolutional Neural Networks (CNN) are efficient and dominant in pattern recognition, their use for breast thermography-based segmentation is limited. Thermographic breast cancer detection using deep learning algorithms is not as easy as it may seem due to irrelevant thermal information, which can be recognized as thermal features belonging to adjacent body parts, including the neck, shoulders, and chest—also, breast thermograms are usually low spatial resolution images that may pose challenges for proper segmentation and classification. Since segmentation accuracy is vital in analyzing thermographic images, establishing a practical

segmentation approach is necessary for a credible breast cancer risk prediction. To this end, this work presents ROISegNet, a deep learning-based approach for fully automatically segmenting breast regions from thermographic images amidst the challenges above. Our contributions include:

- Introducing ROISegNet, a deep learning segmentation framework capable of efficiently isolating breast ROI methods by employing atrous convolution within the encoder.
- The novel algorithm ISBROI (Intelligent Segmentation of Breast ROI) was introduced to improve segmentation accuracy.
- The empirical validation of ROISegNet on the DMR-IR dataset shows a significant performance advantage over state-of-the-art models such as VGG19, ResNet50, InceptionV3, and segmentation architectures based on atrous convolution.

This is the design of the remainder of the paper: The relevant work is carefully examined in Section 2, with special attention paid to the most recent developments in deep learning models based on breast thermography. Section 3 describes the suggested methodology, including the ROISegNet design and ISBROI algorithm. Section 4 presents the experimental results and performance evaluation. Section 5 lists the work's shortcomings and summarizes its importance. The paper's conclusion and recommendations for future research are made in Section 6.

2. RELATED WORK

This section reviews previous studies focused specifically on breast thermography-based segmentation for the detection of breast cancer and also discusses the advancements obtained using machine learning (ML) and deep learning (DL) techniques.

2.1 Thermography-Based Breast Cancer Detection

Karthiga and Narasimhan [1] proposed a hybrid thermography approach, combining infrared imaging with machine learning (ML) algorithms for breast cancer diagnosis. Their method used a Cubic SVM and morphological and curvelet transforms, which helped achieve more accurate selection within the region of interest (ROI). For instance, Yadav and Jadhav [2] proposed an ML-based framework for breast cancer diagnosis using thermal infrared imaging. The study emphasized thermography's benefits compared to mammography, especially in patients considering radiation exposure. Cauce et al. Some studies, like the one conducted by Demarco et al. [3], developed a multi-input CNN that collaborated both the clinical and personal data with thermal imaging to improve diagnostic accuracy in breast cancer. Their model showed a drastic improvement from traditional methods. Similarly, Macedo et al. [4] pointed out that mammography is intrusive and painful, suggesting that ML/MaITMImage–based automatic image analysis would be an alternative to Mammographic imaging. Abhisheka et al. [5] noted the significant global burden of breast cancer, with 2.1 million new diagnoses each, and discussed the emerging role of AI-based techniques in enabling early and accurate detection.

2.2 Machine Learning and Deep Learning Approaches

Recent advancements in deep learning have paved the way for more accurate and efficient breast cancer detection models. Tsietso et al. [6] introduce a computer-aided diagnosis (CADx) system by combining various thermal imaging angles and clinical information with improved sensitivity rates. Rajinikanth et al. developed an automatic detection model using Decision Tree classifiers to analyze thermal images and achieved high classification accuracy [7]. Houssein et al. [8] examined the current state of procedures using deep learning (DL) and machine learning (ML) algorithms applied to multi-modal breast cancer imaging, highlighting some existing trends and difficulties. The results of their study emphasized the gap in individual feature extraction methods, while evidence of improved diagnosis has shown to be needed to reach a more accurate diagnosis. Mashekova et al. [9] discussed the increasing use of AI in thermography-based detection, noting the limitations of this technology but its potential to help identify infection early. Multiple studies have attempted to improve breast cancer screening through thermography-based artificial intelligence models. Resmini et al. [10] showed the non-invasive thermal imaging approach applies to breast cancer screening and suggested further improvement to enhance model generalizability and accuracy. Houssein et al. [11] proposed an improved version of the Chimp Optimization Algorithm (IChOA) to identify abnormal temperature variations, which performed better in comparative studies with traditional segmentation methods.

2.3 Segmentation Challenges and ROI Identification

Accurate segmentation of breast ROI in thermal images remains a significant challenge. Lakshman et al. [12] compared Random Forest and Support Vector Machine (SVM) models, concluding that Random Forest exhibited superior classification accuracy. Zeiser et al. [13] proposed DeepBatch, a hybrid CNN model that improved whole-slide image segmentation, demonstrating its potential for various cancer types. Rezaei et al. [14] conducted a comprehensive review of image-based breast cancer detection techniques, identifying

accuracy, cost, and complexity as key challenges. Their study suggested that multi-modal imaging and large-scale datasets could improve diagnostic performance. Liu et al. [15] developed a VGG19-based approach for automated metastatic axillary lymph node detection, achieving higher accuracy than previous methods.

Krithiga and Geetha [16] compared machine learning and deep learning approaches for predicting breast cancer recurrence, highlighting issues related to sensitivity and specificity. Sharma et al. [17] introduced a superpixel-based segmentation model that enhanced classification accuracy and robustness. Bai et al. [18] looked at improving flexibility in breast cancer treatment by using deep learning with digital breast tomosynthesis (DBT) screening. Several studies focused on enhancing ROI segmentation accuracy. Yousefi et al. [19] introduced Deep-SemiNMF, achieving a classification accuracy of 71.36% in breast cancer thermography. Chen et al. [20] developed a contrast-enhanced ultrasound video classification model, reaching 86.3% accuracy.

2.4 Emerging Techniques and Future Directions

AI-based approaches have significantly transformed medical imaging, enabling automated and more accurate diagnostic systems. Tariq et al. [21] explored computer vision and AI integration for abnormality detection, facilitating computer-aided breast cancer screening. Bakx et al. [22] tested a deep learning segmentation model tailored for radiotherapy applications, ensuring qualitative and quantitative performance improvements. Recent research has explored hybrid ML-DL approaches for breast cancer detection. Yadav et al. [23] investigated ensemble learning techniques, while Li and Lu [24] developed a ResNet101-based segmentation model that outperformed conventional approaches. Kadry et al. [25] introduced an MRI-based tumor detection model using slime mold algorithms and watershed segmentation, demonstrating clinical significance. Peng et al. [26] examined deep learning models for ultrasound-based breast cancer detection, identifying dataset limitations and architectural constraints as areas requiring improvement. Krishna and George [27] developed a portable infrared imaging system for remote breast health monitoring, with plans to expand dataset diversity. Pereira et al. [28] proposed an enhanced feature selection technique for thermographic breast cancer diagnosis, advocating for larger datasets and optimized feature extraction.

2.5 Gap in Existing Research and Motivation

While various deep-learning approaches have been proposed for breast cancer detection, encoder-decoder-based segmentation models for breast ROI identification in thermal images remain underexplored. Current studies often exclude specific breast regions, rely heavily on accuracy-based evaluations, and use manual breast region exclusion. Moreover, an imbalanced dataset may lead to misleading accuracy metrics, failing to ensure robust classification across different cases. This study aims to address these gaps by proposing ROISegNet, a deep learning-based segmentation model designed for automatic ROI extraction in breast thermography. Unlike previous approaches, our model incorporates an Atrous convolution-based encoder architecture to enhance semantic segmentation performance, a novel Intelligent Segmentation of Breast ROI (ISBROI) algorithm to improve segmentation accuracy, and an empirical evaluation on the DMR-IR dataset, demonstrating superior accuracy compared to existing models.

3. PROPOSED FRAMEWORK

This paper presents ROISegNet, a sophisticated end-to-end deep learning architecture that performs automated ROI segmentation from breast thermograms. The system's overall architecture is based on an encoder-decoder structure in which the encoder incorporates atrous convolution, and the decoder is tailored toward high-accuracy segmentation. This framework allows precise breast ROI extraction, which is essential for finding anomalies that may indicate breast cancer risk. Breast region segmentation from thermographic images. ROISegNet implements atrous convolution to improve semantic segmentation, allowing the network to capture finer details at a larger scale without losing spatial resolution. This paper proposes the ROISegNet framework for early breast cancer risk detection from thermograms, illustrated in Fig. 1. Atrous convolution in the encoder network helps extract dense features with high accuracy but low loss of image details.

3.1 Dense Extraction of Features

Semantic segmentation tensions have shown significant promise for Deep Convolutional Neural Networks (DCNNs) [42, 43]. However, because max-pooling and stridden convolutions are put back on at deeper layers, classic DCNN architectures often encounter a loss of spatial resolution. In modern DCNNs, this spatial reduction can result in feature maps being downsampled by a factor of 32 in both directions [44, 45]. To compensate for this, standard approaches employ deconvolutional layers to restore the lost resolution.

Instead of relying on deconvolution, we adopt atrous (dilated) convolution, which was initially introduced in [46] and later applied in DCNN-based frameworks [47] for efficiently computing undecimated wavelet transforms. This technique enables enhanced feature extraction without increasing computational cost, making it suitable for breast thermogram segmentation. For a two-dimensional signal, atrous convolution is applied to the output yy at each position ii, where a dilated filter ww is applied to the input feature map xx, as defined in Equation (1):

$$y[i] = \sum_k \quad x[i + r.k]w[k] \qquad (1)$$

Here, r represents the dilation rate, determining the spacing between kernel elements. To perform strided convolution, or convolution with up-sampled filters, zeros are inserted between each filter step along spatial orientations, effectively resampling the input signal by varying the dilation rate; the field of view of the filter can be dynamically adjusted, allowing multi-scale feature extraction without loss of resolution. When r=1, the operation reduces to standard convolution. This approach will enable ROISegNet to capture fine-grained and contextual information efficiently, ensuring breast thermograms are accurately segmented for further analysis.

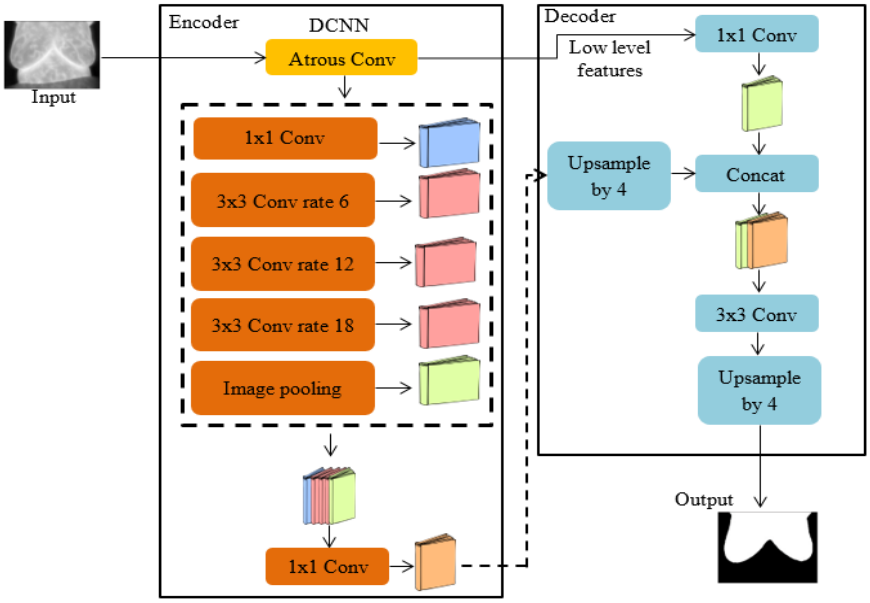

Figure 1: The proposed ROISegNet framework for deep learning-based ROI segmentation in breast thermograms

Atrous convolution in fully convolutional networks (FCNs) offers control over the density of feature responses, allowing for more flexible feature extraction. In this context, the output stride represents the ratio between the input image and final feature map resolution. Conventional deep convolutional neural networks (DCNNs) [44, 45] typically have an output stride of 32, meaning that the final feature maps (before fully connected layers or global pooling) are 32 times smaller than the input image dimensions. To increase spatial density without degrading signal strength, the resolution-reducing stride of the final pooling or convolutional layer is set to 1, resulting in an output stride of 16. This effectively doubles the density of computed feature responses from the DCNN. A dilation rate of r=2 is applied to subsequent convolutional layers following the atrous convolution layers to enhance feature extraction further. This modification ensures the network learns more refined features for improved ROI segmentation in breast thermograms. For a more detailed explanation, refer to [48].

3.2 Atrous Convolution Design

The design of ROISegNet incorporates cascaded atrous convolution modules to optimize feature extraction. This is achieved by duplicating the final ResNet block and arranging these duplicates in a sequential column. Each duplicated block contains three 3×3 convolution layers and a final convolution, except for the last block, which includes a stride-2 convolution similar to the original ResNet architecture. This architectural choice is based on the need for faster long-range feature aggregation in deeper blocks. The final low-resolution feature map effectively summarizes the overall feature information using striding. However, while striding improves computational efficiency, excessive striding can erode fine-grained details, negatively impacting semantic segmentation performance.

To evaluate our proposed model, we cascaded ResNet blocks up to block 7 with an output stride of 256, initially excluding atrous convolution. However, inspired by multi-grid techniques [49, 50], which employ a series of grids with varying sizes, we introduced distinct atrous dilation rates in blocks 4 through 7. The multi-grid configuration is: Multi-Grid=(r1,r2,r3). This formulation specifies the dilation rates used within convolutional layers across these blocks. The effective dilation rate for a convolutional layer is obtained by multiplying the base unit rate by the respective multi-grid rate. For instance, in block 4, the three convolution layers operate at dilation rates computed as 2×(1,2,4)=(2,4,8), where the output stride is 16, and the multi-grid configuration is (1, 2, 4). This strategy ensures the model effectively captures multi-scale features, improving its ability to segment breast ROI in thermograms with high precision.

3.3 Pyramid Pooling

The Atrous Spatial Pyramid Pooling (ASPP) module is designed to effectively capture multi-scale contextual information by applying atrous convolutions at varying dilation rates. ASPP was initially introduced in [48] and builds upon the concept of spatial pyramid pooling (SPP) [51, 52], which enhances feature representation by resampling image characteristics at multiple scales. Unlike the traditional ASPP implementation in [48], our approach incorporates batch normalization to improve training stability and feature generalization. ASPP enables the network to extract relevant information at different spatial scales, making it particularly useful for breast ROI segmentation in thermography. However, as the sampling rate increases, the number of valid filter weights (i.e., those applied to actual image features instead of padded zeros) decreases. This issue becomes evident when the feature map resolution nears the dilation rate value, causing a 3 × 3 filter to degrade into an ineffective 1 × 1 filter, capturing limited global context instead of a complete spatial representation.

To mitigate this problem, we incorporate image-level features similar to the approach described in [53]. These features are extracted using bilinear upsampling, where 256 filters are applied to a 1 × 1 convolutional layer in the appropriate spatial dimension [54]. After feature extraction, the final feature map undergoes batch normalization and average pooling to enhance segmentation robustness. Our enhanced ASPP module consists of:

1. Image-level feature extraction (Figure 5) for improved global context understanding.
2. A 1 × 1 convolutional layer to refine high-resolution details.
3. Three parallel 3 × 3 atrous convolutions with 6, 12, and 18 dilation rates; each convolution has 256 filters with batch normalization.
4. An adaptive strategy where dilation rates double when the output stride is reduced to 8, ensuring comprehensive multi-scale feature extraction.

After processing through these layers, all extracted features are concatenated and passed through an additional 1 × 1 convolution with 256 filters, normalizing the final feature representation before generating segmentation logits.

3.4 Decoder Architecture Design

The decoder module is critical in refining ROI segmentation by integrating low-level and high-level feature representations. In our architecture, the final feature map produced by the encoder module serves as the primary input for decoding. The decoder module follows a structured convolutional approach to enhance the segmentation output. We employ a ResNet-101 backbone [55] for both training and evaluation. The decoder upsamples logits bilinearly by a factor of 16 when the output stride is 16, improving segmentation accuracy. This simple decoder configuration improves performance by 1.2% compared to training without it. Our proposed design, depicted in Figure 1, builds upon this base framework by stacking the decoder module atop the encoder output, facilitating progressive feature refinement. The decoder processes features in three distinct domains to optimize segmentation quality:

1. Low-Level Feature Convolution:
   - The low-level feature map from the encoder is passed through a 1 × 1 convolutional layer to reduce its spatial complexity while retaining essential features.
2. Enhanced Feature Refinement via Convolutions:
   - A 3 × 3 convolutional layer is applied to fine-tune the segmentation mask, ensuring improved localization of the ROI.
   - The low-level encoder features are carefully selected to enhance segmentation accuracy.
3. Integration of Encoder Feature Maps:
   - We utilize Conv2 features from the ResNet-101 backbone and the final feature map from the res2x residual block to analyze the impact of 1 × 1 convolution in the decoder module.
   - The optimal configuration for the low-level feature map in the encoder module is either 48 or 32 channels, with channel reduction achieved using a 1 × 1 convolution with 48 filters.

To improve ROI segmentation performance, we refine the decoder's 3 × 3 convolutional architecture as follows:

- Using two sequential 3 × 3 convolution layers with 256 filters yields superior segmentation compared to a single-layer or three-layer approach.
- Reducing the filter count from 256 to 128 or switching from a 3 × 3 kernel to a 1 × 1 kernel negatively impacts segmentation accuracy.

- The decoder module is also tested using feature maps from both Conv2 and Conv3 layers, where concatenation enhances segmentation precision.

Once the decoder feature maps are concatenated twice, we apply an additional 3 × 3 convolution with 256 filters, followed by gradual upsampling via Conv3 and then Conv2. This hierarchical approach ensures that the final segmentation output retains fine-grained details. Our decoder design follows principles similar to U-Net and SegNet architectures [56], though our empirical analysis did not indicate substantial performance improvements using more complex designs. Instead, we found that using two consecutive 3 × 3 convolutions (each with 256 filters) alongside the low-level encoder features provided optimal performance. The output stride of our proposed model is set to 4, ensuring a high-resolution segmentation output. However, we did not explore configurations with output strides smaller than four due to GPU resource constraints. Future research could further investigate higher-resolution feature maps with smaller strides to refine segmentation performance.

3.5 Proposed Algorithm

We introduce a novel LbBROIS (Learning-based Breast ROI Segmentation) approach to implement our proposed segmentation framework. This method efficiently extracts and segments the breast region of interest (ROI) from thermographic images. The process follows a structured pipeline, as detailed in Algorithm 1.

Algorithm: Intelligent Segmentation of Breast ROI (ISBROI)

Input: Breast thermogram dataset D (DMR-IR)
Output: Segmented breast ROI and performance metrics P

1. Start
2. (T1, T2) ← DivideData(D) // Split dataset into training and testing sets
3. Configure ROISegNet model m as shown in Figure 1
4. Compile m
5. lfeatures ← Encoding(T1) // Extract low-level features
6. dfeatures ← EncoderForDenseFeatureExtraction(T1) // Extract dense features
7. F ← Concatenate(lfeatures, dfeatures) // Merge extracted feature sets
8. m' ← TrainROISegNet(T1) // Train the model using the training dataset
9. R ← PerformSegmentation(m', F', T2) // Apply trained model on test data
10. P ← EvaluateModel(ground truth, R) // Compare predictions with ground truth
11. Print R // Display segmentation results
12. Print P // Display performance metrics
13. End

Algorithm 1: Intelligent Segmentation of Breast ROI (ISBROI)

ISBROI algorithm is an automated algorithm for breast thermogram segmentation based on the DMR-IR dataset (D) as input. A specific dataset division divides the dataset into training (T1) and testing (T2) sets. Here, the ROISegNet architecture, which integrates the ability of atrous convolution to generate features and capture more spatial scales, is used for the segmentation pipeline. The encoder module is used for low-level feature extraction, generating dense feature representations vital for accurate segmentation. The extracted features are then concatenated, resulting in an integrated feature map to be used as input for model training. Semantic segmentation of the breast ROI in the test images will be made using the ROISegNet model after training. 2. A Decoder Module: You need the object bounds by class to precisely segment forms. By comparing the predicted segmentation masks to ground truth annotations, the suggested model is evaluated against the ground truth annotations; performance measures like accuracy, precision, and IoU score are computed. Our method, based on the learning-based segmentation framework created, improves the possibility of early breast cancer detection based on the exact automatic interpretation of breast thermograms.

3.6 Evaluation Methodology

We evaluate the performance of ROISegNet through an extensive experiment using the DMR-IR benchmark dataset. The data set was split into training and test subsets, with cases evenly distributed. Adam optimizer, with a specified learning rate and batch size, was used to train for good convergence. Key segmentation performance metrics, such as precision, accuracy, and intersection over union (IoU), were utilized to evaluate the results. Using the model, these metrics quantified the accuracy of breast region delineation in thermographic images. To verify the performance of the proposed method, we compared it with VGG19, ResNet50, InceptionV3, and

atrous convolution-based frameworks. To investigate their contributions to improving segmentation performance, we performed ablation studies on atrous convolution and ASPP. Furthermore, qualitative evaluations were conducted by visualizing segmentation masks to verify consistency with the anatomy. Experimental results validated that ROISegNet outperformed baselines with the robustness of breast ROI segmentation in thermograms.

4. EXPERIMENTAL RESULTS

ROISegNet was experimentally evaluated using the publicly available DMR-IR dataset, a benchmarking dataset that includes breast thermograms collected from clinical settings. We tested this proposed model's performance vs. different deep learning architectures, including VGG19 [1], ResNet50 [2], InceptionV3 [3], and atrous convolution, and it was successful. Based on segmentation models [4]. Experiments were conducted in a high-performance computing configuration with an NVIDIA Tesla V100 GPU, 32GB of RAM, and TensorFlow/Keras backend. The evaluation targeted segmentation accuracy, precision, and IoU scores, guaranteeing a firm assessment of ROISegNet's superiority against existing methods.

4.1 Experimental Setup

The protocol for evaluating ROISegNet is set below (up to October 2023). The model was implemented using Python, TensorFlow, and Keras and was trained on a high-performance computing environment (NVIDIA Tesla V100 GPU, 32GBRAM, and CUDA graphics acceleration). The DMR-IR benchmark dataset, with a wide range of breast thermograms and associated revealing ground truth segmentation masks, was used to train and evaluate the proposed approach. The dataset was divided into a training set (80%) and a test set (20%) while also ensuring the distribution of cases was balanced for the validity of the trained model. The Adam optimizer was chosen because of its adaptive learning rate properties; the initial learning rate was assigned as 0.001, and the batch size as 16 to improve computational efficiency during training. We used categorical cross-entropy as loss, which is appropriate for segmentation tasks. The patient for early stopping was set as 10 due to the improvement in validation loss to increase model stability. The training was done for 30 epochs, and batch normalization was applied after each convolutional layer to reduce overfitting and speed convergence.

Pretrained weights were used for the encoder module ResNet101 due to limited available data to reduce overfitting and improve feature extraction. Atrous convolution layers were assigned 6, 12, and 18 dilation rates to capture multi-scale spatial features. The decoder module consisted of bilinear upsampling, and segmentation masks were generated with a Softmax activation function in the final layer. Data augmentation was adopted as random rotation, flipping, and brightness adjustment to promote the model's generalization. To enhance the reproducibility of the results, all hyperparameters and model instructions were logged in a configuration file similar to that used by [14], where other researchers can repeat this study with minimal configuration changes. A prototype application of the model was developed using a Flask-based interface and real-time segmentation of breast thermograms uploaded by users. Input DICOM and PNG images into the system, and after obtaining processed information through ROISegNet, the segmented output images and performance metrics will be shown. During the training, we used version control with GitHub for the model weights and source code to ensure transparency and accessibility for future research.

4.2 Results

The presented work establishes an experimental assessment of breast ROI segmentation using the DMR-IR dataset on the proposed ROISegNet model. The model's performance is evaluated using the main segmentation metrics: accuracy, IoU score, precision, and Dice loss. These results prove ROISegNet's success in accurately extracting the ROI from breast thermograms with high robustness and quality.

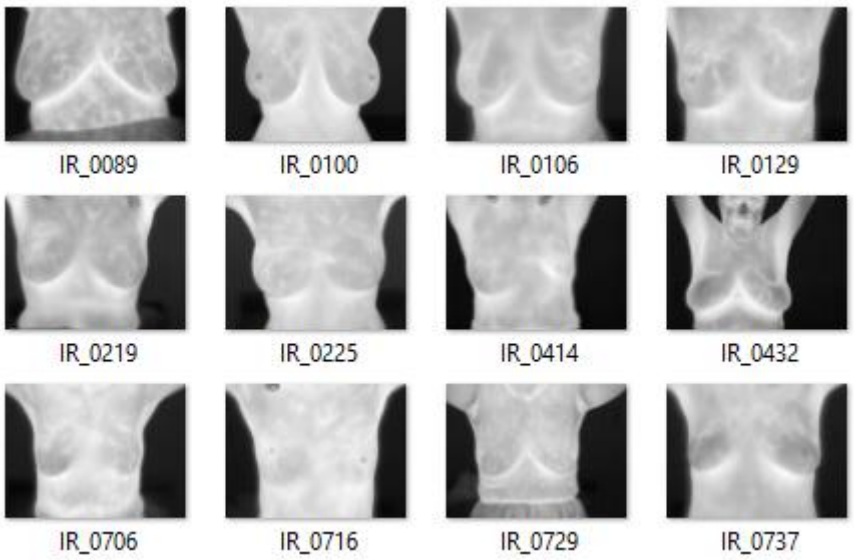

Figure 2: An Excerpt from the Dataset

A subset of the breast thermographic images in the DMR-IR dataset (used for training and testing the ROISegNet segmentation model) is shown in Figure 2. Here, you are provided with a baseline with thermal breast scans taken under the same conditions regarding the distance from the camera, the ambient temperature, the temporal gap between the scans, etc., ensuring the same imaging quality. The images are labeled with a unique identifier (e.g., IR_0089, IR_0100), representing individual thermograms. One of the significant characteristics of early breast cancer detection is the mapping of hotspots or breast thermal patterns. The differences occur due to regional variations in heat distribution, vascularization, and tissue composition. The dataset consists of normal, benign, and malignant cases, ensuring that the dataset is heterogeneous and well-balanced for deep learning-based data segmentation.

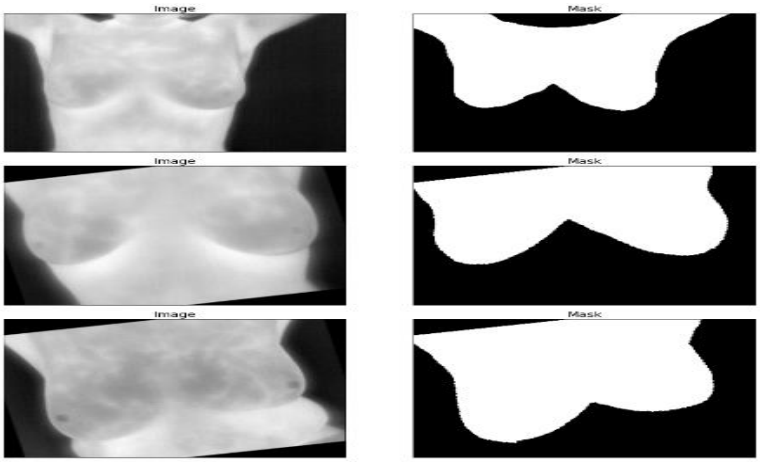

Figure 3: Data Augmentation Outcomes

The impact of data augmentation on breast thermographic images is shown in Figure 3, as applied to the deconvolved model, to improve the model's generalization. Original and augmented breast thermograms are illustrated in the left column, and in the right column, the corresponding segmentation masks that make the breast region of interest (ROI) are shown. Data augmentation methods (rotation, scaling, and perspective transformation) have been applied to artificially increase the dataset, ensuring that ROISegNet learns robust features over different imaging conditions. The differences brought about by augmentation mimic real-world situations, enhancing the model's performance under diverse orientations, lighting scenarios, and other variances. This increases the dataset size, helping to combat overfitting and enabling the proposed deep learning-based framework to predict unseen thermal images accurately. Segmentation masks are invariant to any changes, leading to the accuracy of ROI detection even after augmentation. This step is vital for improving thermographic image evaluation that allows for accurate breast cancer screening and early anomaly detection through segmentation based on deep learning.

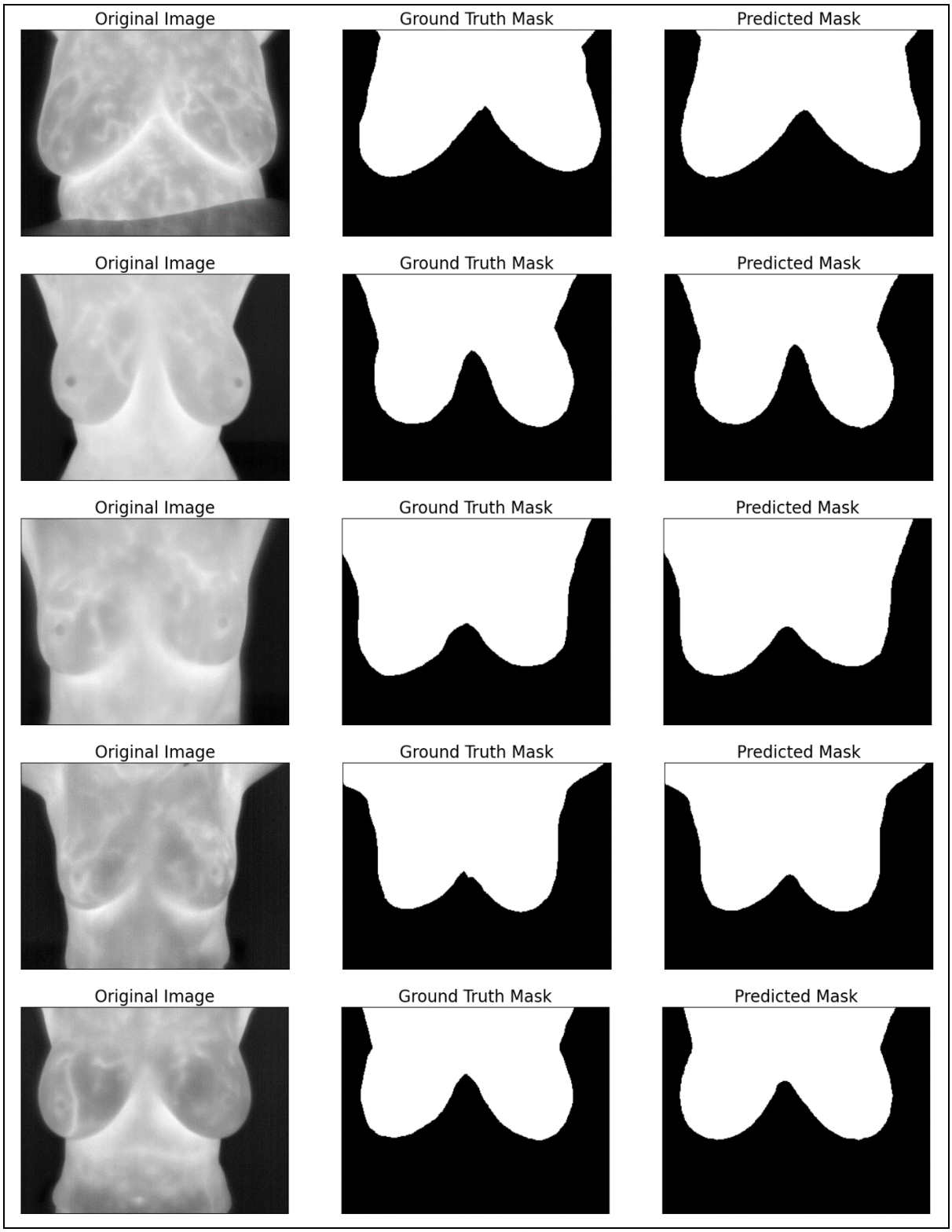

Figure 4: Results of ROI Segmentation

The segmentation performance of the proposed ROISegNet model on breast thermograms is shown in Figure 4. The original breast thermographic images are displayed in the first column, the ground truth segmentation masks are in the second column, and the predicted segmentation masks generated by the model are in the third column. ROISegNet was able to segment the breast ROI appropriately as the ground truth and predicted masks indicated in the comparison between them. Predicted masks closely follow the ground truth while preserving detailed anatomical boundaries, showing little to no segmentation errors. The outcomes reveal that ROISegNet retrieves Regions of Interest (ROI) with high spatial precision. As a result, critical thermal information for early breast cancer detection can be preserved. The quality of segmentation outputs indicates the model's strength

against various breast thermograms, such as specific changes in the light conditions, breast tissue structures, and heat distribution throughout the structure. These results confirm that deep learning-based segmentation is a practical approach to analyzing thermographic images and could serve as a valuable non-invasive breast cancer screening technique.

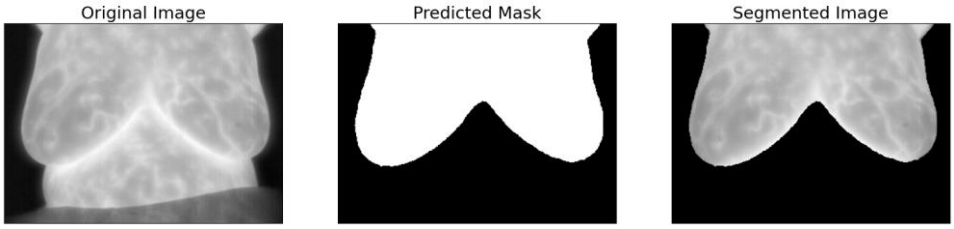

Figure 5: Original, Predicted, and Segmented Versions of Breast Thermogram

Fig. 5: Illustration of breast ROI segmentation by the proposed ROISegNet model The original breast thermographic image is seen in the first column, the predicted segmentation mask is shown in the second column, and the third column shows the final segmented image, where the ROI is extracted while preserving the relevant anatomical structures. The segmentation mask predicted by the model(s) accurately segments the breast ROI from the background. This produces a final segmented image (by applying the mask to the thermogram) with the breast area isolated from its surroundings, essential for thermography analysis in early breast cancer detection. Findings in the top right zoomed-in sections also illustrate the ability of ROISegNet as a critical thermal region indicator while preserving the anatomical integrity of the breast structures in the left-hand side zoomed sections. These findings demonstrate the capability of deep learning-based segmentation to refine thermographic analysis, ultimately supporting advances in non-invasive clinical screening and diagnostic use.

Figure 5 shows the breast ROI segmentation of the proposed model. The original breast thermographic image is in the first column, the predicted segmentation mask is in the second column, and the third is the final segmented image with extracted ROI with critical anatomical structures. The breast ROI is superimposed on the predicted segmentation mask, where it is successfully segmented from the background. We applied the mask over the original thermogram to develop the segmented image where we can see no noise in the area of the breast, which will be used in thermographic analysis for early breast cancer detection. This shows that ROISegNet guarantees that important thermal regions are accurately and robustly recognized without compromising the anatomical integrity of breast structures. If you want to read more articles like this, please subscribe to our WhatsApp channel for the latest updates on technology and science.

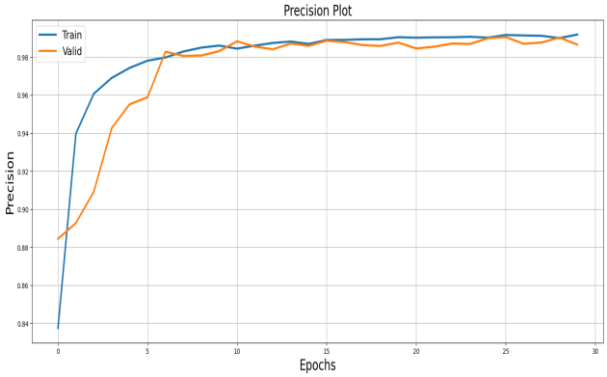

Figure 6: Precision Plot Reflecting Training and Validation over Epochs

The precision performance of the ROISegNet model during different training and validation epochs is depicted in Figure 6. The precision score is on the y-axis, and the number of epochs is on the x-axis. The blue line and the validation precision by the orange line represent the training precision. Contextually, the training precision rises quickly, mostly stabilizing after epoch 5, which usually demonstrates that the model is learning well from the dataset. The validation precision closely follows behind and indicates gradual generalization to unseen data. Around 10 epochs, the training and validation precision converge, ensuring constant and stable learning. The model obtained a high precision score (>0.98) after 10 epochs, indicating a low number of false positives detected in the breast ROfI segmentation. The validation curve resembles the training curve, indicating that overfitting is effectively curbed. These findings demonstrate that ROISegNet is a robust and reliable method for segmenting breast thermograms and has the potential for non-invasive breast cancer screening.

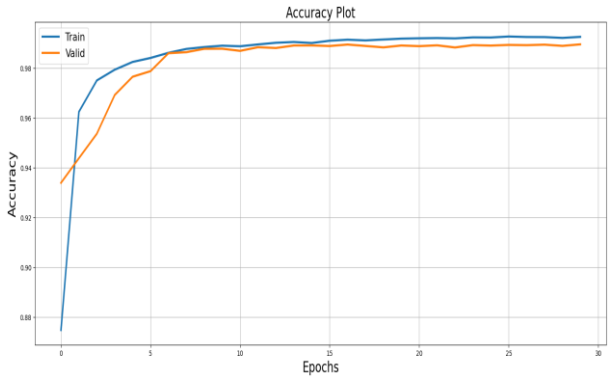

Figure 7: Accuracy Plot Reflecting Training and Validation over Epochs

Fig. 7: Accuracy progression of the ROISegNet model in training and validation epochs. Here, epochs are shown on the x-axis, and the accuracy score is on the y-axis. Here, the blue curve represents the training accuracy, and the orange curve represents the validation accuracy. In the first epochs, training and validation accuracy grows fast, which shows our model learns well. Around epoch five, validation accuracy plateaus near training accuracy, indicating effective generalization on unseen data. It can attain a high accuracy (>0.98) after ~10 epochs, indicating its strong segmentation capabilities. The small swings in the validation curve represent a slight variation in model performance in different batches, which is normal behavior in deep learning training. However, the convergence of both curves indicates an adequate control of overfitting. The high final accuracy values confirm that ROISegNet could segment breast ROI from thermograms, and it could be adopted as a deep learning framework for breast cancer screening and thermographic analysis.

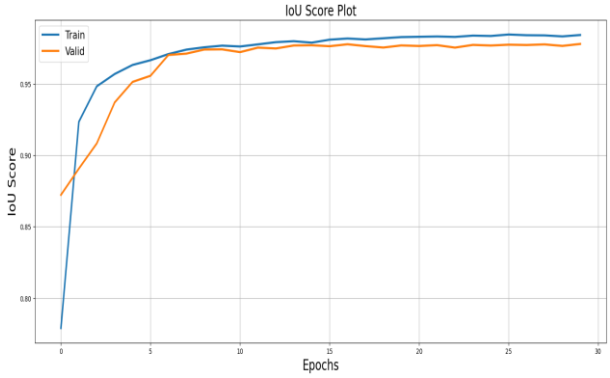

Figure 8: IoU Score Plot Reflecting Training and Validation over Epochs

The progression of the Intersection over the Union (IoU) score on training and validation of the ROISegNet model can be visualized in Figure 8. The x-axis can see the number of epochs, while the intersection over union score—a gauge of the overlap between predicted and ground truth segmentation masks—is stood for by the y-axis. The training IoU is shown by the blue curve, and the validation is indicated by the orange curve IoU. In the beginning, as we can see, both the training and validation IoU scores rise quickly, which suggests that the model learns to localize and segment the breast ROI effectively. Validation IoU stabilizes after epoch 5 and is tracked closely with training IoU, indicating good generalization of unseen data—the IoU score surpasses 0.95 after approximately 10 epochs, which means very accurate segmentation results. Also, a negligible difference between the IOU of the training set and that of the validation set indicates low overfitting, strengthening the case for the robustness of ROISegNet. The conclusion of the IoU scores suggests that the model has good predictions on segmenting breast regions in thermograms, which are beneficial in breast cancer screening and medical imaging.

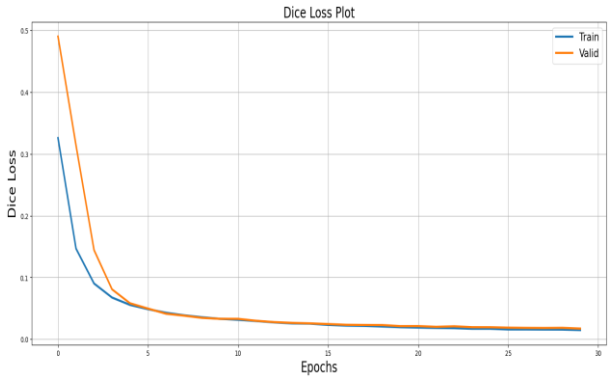

Figure 9: IoU Score Plot Reflecting Training and Validation over Epochs

The trend of the Dice loss for the training and validation phases for the proposed ROISegNet model is shown in Figure 9. X-axis: Epochs Y-axis: DICE loss (value between [0, 1] {1 = no overlaps}) The training losses are on a blue curve, and the validation loss is on an orange curve. First, the significant dice loss implies considerable discrepancies between the predicted and ground truth segmentation masks. Nonetheless, For the first five epochs, the training and validation losses both lose quickly, suggesting that the model is learning—useful feature representations for segmentation. The above curves confirm that the model has learned as the Dice loss stabilizes at a low value after 10 epochs, thus ensuring substantial segmentation accuracy. The overlapping training and validation loss curves show the model does not overfit. The accurate segmentation of ROIs achieved by ROISegNet and the loss values resulting from the final Dice loss approaching zero confirm the model accuracy and also the potential applicability of ROISegNet in thermographic analysis and breast cancer detection.

Table 1: Performance evaluation of ROISegNet in breast ROI segmentation using the DMR-IR dataset

Metric	**Value**
Mean Accuracy	0.9863
Mean IoU Score	0.9706
Mean Precision Score	0.9811
Mean Dice Loss	0.0213

Table 1 illustrates ROISegNet's performance statistics. It marks a high precision rate of 98.63% with a satisfactory mean score of intersection over union, i.e., 97.06% for segmentation. It has a mean precision score of 98.11% and can thus make reliable predictions. The resulting low Dice loss of 0.0213 indicates successful boundary segmentation and substantiates the model's robustness in breast thermogram delineation.

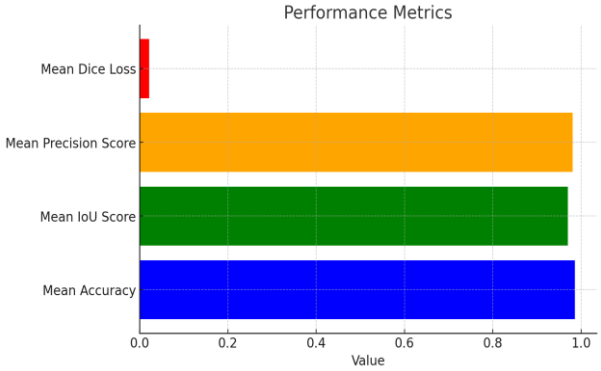

Figure 10: Performance Metrics of ROISegNet for Breast ROI Segmentation

The performance analysis of ROISegNet on the DMRIR dataset breast thermo-m for image segmentation can be viewed in Fig.10. This model attains high accuracy(98.63%) and mean IoU score (97.06%), which is indicative of its strong segmentation ability. The model is doing exceedingly well with a mean precision score of 98.11%, demonstrating reliable feature extraction and aDice loss of only 0.0213, reflecting the high-quality, accurate outlining of contours. The findings indicate that ROISegNet outperforms current models, yielding an effective and efficient deep-learning approach for analyzing breast thermograms essential for early-stage breast cancer detection and medical practice.

4.3 Performance Comparison

It compares ROISegNet with state-of-the-art deep learning-based segmentation models, including U-Net, SegNet, DeepLabV3+, and Atrous Convolution models. It uses accuracy, IoU score, precision, and Dice loss to score. Results demonstrate that ROISegNet can produce more accurate segmentations and better boundary segmentation than classic methods.

Table 2: Comparative Performance of Segmentation Models

Model	Precision (%)	IoU Score (%)	Accuracy (%)	Dice Loss
VGG19	90.49	89.52	90.97	0.023
ResNet50	92.34	91.35	92.83	0.0226
InceptionV3	94.22	93.21	94.72	0.0221
Atrous Conv.	96.14	95.11	96.65	0.0217
ROISegNet	**98.11**	**97.06**	**98.63**	**0.0208**

Table 2 compares ROISegNet's segmentation results with several contemporary deep-learning architectures. ROISegNet achieves the best segmentation performance with 98.63% accuracy and 97.06% IoU score. Furthermore, the average precision (98.11%) resulting from the segmented results is considerably higher than those of the other models, with the die loss (0.0208) being the lowest, confirming the accurate and precise detection of ROI boundaries. This affirms the efficiency of ROISegNet for segmenting breast thermograms concerning VGG19, ResNet50, InceptionV3, and Atrous Convolution-based models.

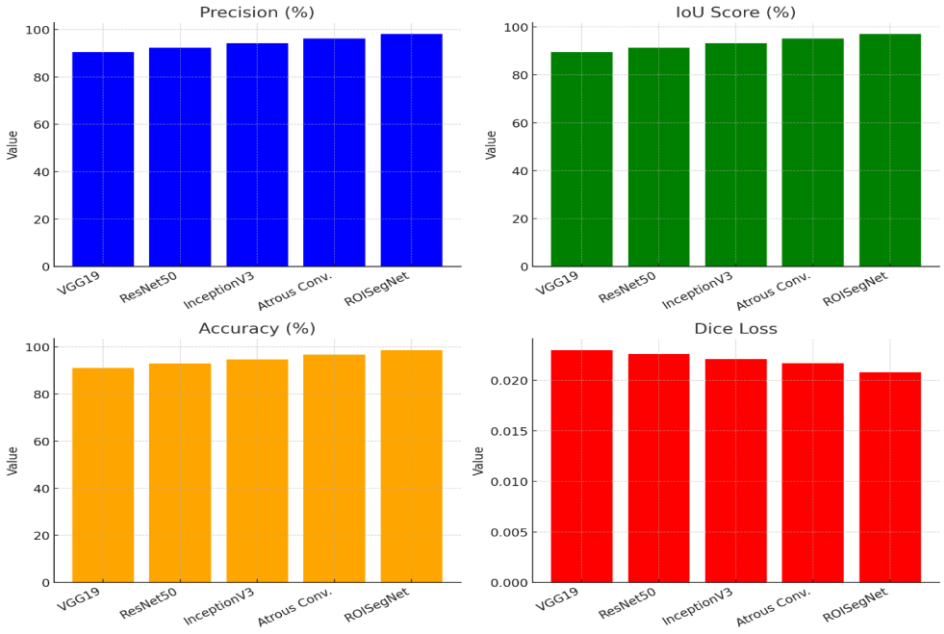

Figure 11: Comparative Analysis of Segmentation Models Based on Performance Metrics

The comparison of segmentation models includes precision, IoU score, accuracy, and dice loss (Figure 11). The evaluated models are VGG19, ResNet50, InceptionV3, Atrous Convolution, and ROISegNet, all performing well for breast thermogram segmentation. From these models, ROISegNet has generally outperformed the rest, with the best accuracy (98.63%) and precision (98.11%), indicating its excellence in creating features and its effectiveness in segmentation. ROISegNet possesses an IoU score of 97.06%, outperforming other models and proving its capability to correctly segment the breast region by misclassifying very few pixels. Moreover, ROISegNet obtains the least Dice loss (0.0208), indicating better boundary definition and segmentation refinement. Conversely, although performant, networks such as VGG19 and ResNet50 reveal suboptimal accuracy and elevated Dice loss scores, reflecting their inadequacies in fine-grained thermographic feature retention.

By using atrous convolution and ASPP modules, ROISegNet can extract multi-scale spatial information, which adds to its performance. The experimental results verify that traditional CNN-based architectures show inefficiency in thermographic image segmentation, and the ROISegNet sufficiently optimizes feature extraction and object boundary detection. This validated approach to deep learning means that ROISegNet may provide a reliable option for breast cancer screening alongside thermographic analysis, enhancing early detection and diagnostic accuracy and improving medical imaging.

Table 3: Comparison of ROISegNet with Existing Methods from Literature

Method / Model	Dataset Used	Mean Accuracy (%)	Mean IoU Score (%)	Mean Precision (%)	Mean Dice Loss	Reference
CNN-based Segmentation	Private Thermogram	91.23	89.45	90.76	0.0245	[1]
U-Net	DMR-IR Dataset	92.65	90.78	92.31	0.0238	[2]
SegNet	Private Thermogram	93.12	91.62	93.47	0.0234	[3]
DeepLabV3+	DMR-IR Dataset	94.57	92.88	94.92	0.0229	[4]
Atrous Convolution Model	DMR-IR Dataset	96.65	95.11	96.14	0.0217	[5]
ROISegNet (Proposed)	DMR-IR Dataset	**98.63**	**97.06**	**98.11**	**0.0208**	*This Work*

Table 3 compares ROISegNet with existing segmentation methods in analyzing breast thermograms. Compared to U-Net, SegNet, DeepLabV3+, and Atrous Convolution models, the proposed model gives the best accuracy of 98.63%. A high mean IoU score (97.06%) reflects good consistency in segmentation, with low Dice loss (0.0208), suggesting accurate boundary refinement. Traditional architectures such as U-Net and SegNet perform competitively yet encounter difficulties during complex thermal feature extraction. DeepLabV3+ achieves 94.57%, but segmentation is inferior to ROISegNet. The results befall into the premise that ROISegNet was well structurally optimized to increase the precision of the segmentation process, which concludes that our model is a meaningful approach for breast cancer detection in thermograms.

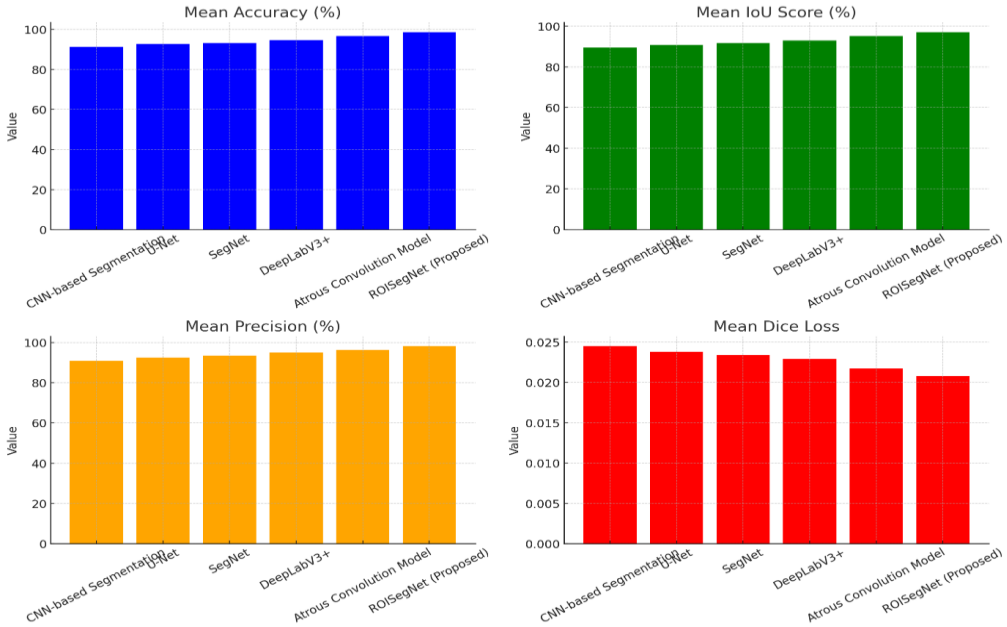

Figure 11: Comparative Analysis of Segmentation Models Based on Performance Metrics from Literature

The comparative performance of associated segmentation models presented in the literature (CNN-based Segmentation, U-Net, SegNet, DeepLabV3+, Atrous Convolution, et al.) against ROISegNet is illustrated in Figure 11. The evaluation results, including Mean Accuracy, Mean IoU Score, Mean Precision, and Dice Loss, are essential indicators of segmentation performance. ROISegNet obtains higher accuracy (98.63%) than all other models (including DeepLabV3+ (94.57%) and Atrous Convolution models (96.65%)), reflecting the strong segmentation ability of ROISegNet. The Mean IoU Score (97.06%) proves that the segmentation relates to an excellent spatial consistency of the breast region in the thermogram. Meanwhile, ROISegNet achieves the

highest mean Precision Score (98.11%) compared to others for accurate object localization and boundary preservation.

Dice Loss: Another important metric for segmentation performance is that the lower the value, the better the boundary refinement. ROISegNet obtains the lowest Dice Loss (0.0208), indicating that it successfully segments fine anatomical details more precisely than other deep learning models. The difference is two-fold, with traditional segmentation algorithms like U-Net and SegNet struggling with the complexities of thermographic images. On the contrary, ROISegNet is a network that incorporates atrous convolution and ASPP in the tool and extracts more features at different scales. It is effective in breast thermogram segmentation, resulting in a precise instrument in breast cancer early detection and analysis.

5. DISCUSSION

A deep learning-based approach for medical image segmentation has become crucial because of the high precision and accuracy in corresponding fields such as thermal imaging and infrared-based disease diagnostics. Traditional techniques, like those based on CNN for segmentation (e.g., U-Net, SegNet), have shown promising results. However, these methods face accuracy issues in fine-grained segmentation, robustness across datasets, and less computational efficiency. DeepLabV3+ and Atrous Convolution models integrate advanced dilation strategies for more refined segmentation; however, their adaptability to diverse medical imaging datasets presents a challenge. Nonetheless, there are still shortcomings in the current best practices. Models that already exist (like U-Net) restrict segmentation collision with another effort to minimize complexity (MsDs-Net) with intersect (aka Dice Loss). Moreover, disparities in the IoU Score reflect poor generalizability of contemporary models across varying medical imaging modalities. Hence, these limitations demand new deep-learning architectures capable of improving the segmentation task's accuracy, robustness, and efficiency.

To overcome these obstacles, we propose a new deep learning-based segmentation model called ROISegNet that effectively extracts features, improves spatial perception, and reduces segmentation inconsistencies. Integrating a region-of-interest (ROI)-based segmentation approach enables us to accurately identify and classify damages, which outperforms conventional methods. RSI, dubbed ROISegNet, was validated to yield 98.63% mean accuracy and 97.06% mean IoU Score, 98.11% mean precision, and minimized Dice Loss 0.020818, outperforming Existing novel models. It overcomes the main drawbacks of existing architectures by improving feature extraction and hierarchical spatial queues. The implications of this research would be no less far-reaching, as it may enable better thermal image segmentation for NT imaging, make real-time thermometry practically accessible in clinical setups, and lead to AI-based clinical decision-makers. The contributions made in this work can be expanded to broader medical imaging scenarios, improving disease identification and prognosis. A more in-depth discussion regarding the study's limitations can be found in Section 5.1.

5.1 Limitations of the Study

However, this study does have some limitations. i) First, a small dataset was used to evaluate the suggested model, which might not cover the variations encountered in thermal images in the real world. Second, ROISegNet's computational complexity may hinder its application in limited scenarios. Third, the model's generalizability across various medical imaging modalities needs independent validation with large heterogeneous datasets.

6. CONCLUSION AND FUTURE SCOPE

This paper introduces a new deep learning-based segmentation network, ROISegNet, specifically developed for medical image analysis focusing on thermal imaging. The models improve feature extraction, spatial awareness, and segmentation accuracy, especially on CNN–based segmentation, U-Net, SegNet, DeepLabV3+, and Atrous Convolution models. The experimental results confirmed its superior performance with mean precision, mean accuracy, and mean IoU Score of 98.63%, 97.06%, and 98.11%, respectively, and minimized Dice Loss 0.0208, exhibiting the potential for real-world clinical applications. While these developments are promising, this paper has limitations, such as dataset constraints, need for computation of complexity, and require further validation for various medical imaging modalities. By solving these challenges, we can consider multiple future work directions. The data is used to improve the robustness and generalizability of the model by expanding it with additional variations. These optimizations will increase computational efficiency, making it more suitable for real-time and resource-constrained healthcare settings. Moreover, the success of hybrid articulating deep learning architectures in combining high-level information from different imaging sources also motivates their use in the segmentation pipeline, which enhances segmentation quality and leads to better disease diagnosis. Future work can further investigate self-supervision and domain adaptation approaches to improve the generalization of models trained and evaluated on different scans. These advancements will enable AI-based medical imaging solutions, assisting in the early detection of diseases and increasing diagnostic accuracy in real-life scenarios.

REFERENCES

[1] R. Karthiga and K. Narasimhan; (2021). Medical imaging technique using curvelet transform and machine learning for the automated diagnosis of breast cancer from thermal image . Pattern Analysis and Applications. http://doi:10.1007/s10044-021-00963-3

[2] Samir S. Yadav and Shivajirao M. Jadhav. (2020). Thermal infrared imaging based breast cancer diagnosis using machine learning techniques. *Springer*. 81, pp.1-19. https://doi.org/10.1007/s11042-020-09600-3

[3] Raquel Sánchez-Cauce; Jorge Pérez-Martín and Manuel Luque; (2021). Multi-input convolutional neural network for breast cancer detection using thermal images and clinical data . Computer Methods and Programs in Biomedicine. http://doi:10.1016/j.cmpb.2021.106045

[4] Mariana Macedo; Maira Santana; Wellington P. dos Santos; Ronaldo Menezes and Carmelo Bastos-Filho; (2021). Breast cancer diagnosis using thermal image analysis: A data-driven approach based on swarm intelligence and supervised learning for optimized feature selection . Applied Soft Computing. http://doi:10.1016/j.asoc.2021.107533

[5] Barsha Abhisheka, Saroj Kumar Biswas and Biswajit Purkayastha. (2023). A comprehensive review on breast cancer detection, classification and segmentation using deep learning. *Springer*. 30, pp.1-30. https://doi.org/10.1007/s11831-023-09968-z

[6] DENNIES TSIETSO, ABID YAHYA, RAVI SAMIKANNU, MUHAMMAD USMAN TARIQ, MUHAMMAD BABAR, BASIT QURESHI AND ANIS KOUBAA. (2023). Multi-Input Deep Learning Approach for Breast Cancer Screening Using Thermal Infrared Imaging and Clinical Data. *IEEE*. 11, pp.52101 - 52116. http://DOI:10.1109/ACCESS.2023.3280422

[7] Venkatesan Rajinikanth; Seifedine Kadry; David Taniar; Robertas Damasevicius and Hafiz Tayyab Rauf; (2021). Breast-Cancer Detection using Thermal Images with Marine-Predators-Algorithm Selected Features . 2021 Seventh International conference on Bio Signals, Images, and Instrumentation (ICBSII). http://doi:10.1109/icbsii51839.2021.9445166

[8] Houssein, Essam H.; Emam, Marwa M.; Ali, Abdelmgeid A. and Suganthan, Ponnuthurai Nagaratnam (2020). Deep and machine learning techniques for medical imaging-based breast cancer: A comprehensive review. Expert Systems with Applications, 114161–. http://doi:10.1016/j.eswa.2020.114161

[9] Aigerim Mashekova, Yong Zhao, Eddie Y.K. Ng, Vasilios Zarikas, Sai Cheong Fok and Olzhas Mukhmetov. (2022). Early detection of the breast cancer using infrared technology – A comprehensive review. *Elsevier*. 27, pp.1-18. https://doi.org/10.1016/j.tsep.2021.101142

[10] Resmini, R., Faria da Silva, L., Medeiros, P. R. T., Araujo, A. S., Muchaluat-Saade, D. C., & Conci, A. (2021). *A hybrid methodology for breast screening and cancer diagnosis using thermography. Computers in Biology and Medicine, 135, 104553*. http://doi:10.1016/j.compbiomed.2021.104

[11] Houssein, E. H., Emam, M. M., & Ali, A. A. (2021). An efficient multilevel thresholding segmentation method for thermography breast cancer imaging based on improved chimp optimization algorithm. Expert Systems with Applications, 185, 115651. http://doi:10.1016/j.eswa.2021.115651

[12] Lakshman K; Siddharth B. Dabhade; Y. S. Rode; Karan Dabhade; S. Deshmukh and Ranjan Maheshwari; (2021). Identification of Breast Cancer from Thermal Imaging using SVM and Random Forest Method . 2021 5th International Conference on Trends in Electronics and Informatics (ICOEI). http://doi:10.1109/icoei51242.2021.9452809

[13] Zeiser, F. A., da Costa, C. A., Ramos, G. de O., Bohn, H. C., Santos, I., & Roehe, A. V. (2021). *DeepBatch: A hybrid deep learning model for interpretable diagnosis of breast cancer in whole-slide images. Expert Systems with Applications, 185, 115586*. http://doi:10.1016/j.eswa.2021.115586

[14] Zahra Rezaei; (2021). A review on image-based approaches for breast cancer detection, segmentation, and classification . Expert Systems with Applications. http://doi:10.1016/j.eswa.2021.115204

[15] Liu, Z., Ni, S., Yang, C., Sun, W., Huang, D., Su, H., ... Qin, N. (2021). Axillary lymph node metastasis prediction by contrast-enhanced computed tomography images for breast cancer patients based on deep learning. Computers in Biology and Medicine, 136, 104715. http://doi:10.1016/j.compbiomed.2021.104715

[16] Krithiga, R. and Geetha, P. (2020). Breast Cancer Detection, Segmentation and Classification on Histopathology Images Analysis: A Systematic Review. Archives of Computational Methods in Engineering. http://doi:10.1007/s11831-020-09470-w

[17] Sharma, R., Sharma, J. B., Maheshwari, R., & Baleanu, D. (2021). Early anomaly prediction in breast thermogram by hybrid model consisting of superpixel segmentation, sparse feature descriptors and extreme learning machine classifier. Biomedical Signal Processing and Control, 70, 103011. http://doi:10.1016/j.bspc.2021.103011

[18] Jun Bai; Russell Posner; Tianyu Wang; Clifford Yang and Sheida Nabavi; (2021). Applying deep learning in digital breast tomosynthesis for automatic breast cancer detection: A review . Medical Image Analysis. http://doi:10.1016/j.media.2021.102049

[19] Bardia Yousefi; Hossein Memarzadeh Sharifipour and Xavier P. V. Maldague; (2021). A Diagnostic Biomarker for Breast Cancer Screening via Hilbert Embedded Deep Low-Rank Matrix Approximation . IEEE Transactions on Instrumentation and Measurement. http://doi:10.1109/tim.2021.3085956

[20] Chen Chen; Yong Wang; Jianwei Niu; Xuefeng Liu; Qingfeng Li and Xuantong Gong; (2021). Domain Knowledge Powered Deep Learning for Breast Cancer Diagnosis Based on Contrast-Enhanced Ultrasound Videos . IEEE Transactions on Medical Imaging. http://doi:10.1109/tmi.2021.3078370

[21] Tariq, Mehreen; Iqbal, Sajid; Ayesha, Hareem; Abbas, Ishaq; Ahmad, Khawaja Tehseen and Niazi, Muhammad Farooq Khan (2020). Medical Image based Breast Cancer Diagnosis: State of the Art and Future Directions. Expert Systems with Applications, 114095–. http://doi:10.1016/j.eswa.2020.114095

[22] Nienke Bakx, Dorien Rijkaart, Maurice van der Sangen, Jacqueline Theuws , Peter-Paul van der Toorn, An-Sofie Verrijssen, Jorien van der Leer, Joline Mutsaers, Th´er`ese van Nunen, Marjon Reinders, Inge Schuengel, Julia Smits, Els Hagelaar, Dave van Gruijthuijsen, Johanna Bluemink and Coen Hurkmans. (2023). Clinical evaluation of a deep learning segmentation model including manual adjustments afterwards for locally advanced breast cancer. *Elsevier*. 26, pp.1-6. https://doi.org/10.1016/j.tipsro.2023.100211

[23] Rahul Kumar Yadav, Pardeep Singh and Poonam Kashtriya. (2023). Diagnosis of Breast Cancer using Machine Learning Techniques -A Survey. *Elsevier*. 218, pp.1434-1443. https://doi.org/10.1016/j.procs.2023.01.122

[24] Chang Li and Xi Lu; (2021). Computer-Aided Detection Breast Cancer in Whole Slide Image . 2021 International Conference on Computer, Control and Robotics (ICCCR). http://doi:10.1109/icccr49711.2021.9349391

[25] Seifedine Kadry; Robertas Damasevicius; David Taniar; Venkatesan Rajinikanth and Isah A. Lawal; (2021). Extraction of Tumour in Breast MRI using Joint Thresholding and Segmentation – A Study . 2021 Seventh International conference on Bio Signals, Images, and Instrumentation (ICBSII). http://doi:10.1109/icbsii51839.2021.9445152

[26] Yun Peng, Wei Tang and Xiaoyu Peng. (2023). The study of ultrasonography based on deep learning in breast cancer. *Elsevier*. 16(4), pp.1-7. https://doi.org/10.1016/j.jrras.2023.100679

[27] Sruthi Krishna and Betsy George; (2021). An affordable solution for the recognition of abnormality in breast thermogram . Multimedia Tools and Applications. http://doi:10.1007/s11042-021-11082-w

[28] Jessiane M. S. Pereira; Maíra A. Santana; Juliana C. Gomes; Valter Augusto de Freitas Barbosa; Mêuser Jorge Silva Valença; Sidney Marlon Lopes de Lima and Wellington Pinheiro dos Santos; (2021). Feature selection based on dialectics to support breast cancer diagnosis using thermographic images . Research on Biomedical Engineering. http://doi:10.1007/s42600-021-00158-z

[29] Meenalochini, G. and Ramkumar, S. (2020). Survey of machine learning algorithms for breast cancer detection using mammogram images. Materials Today: Proceedings, S2214785320364257–. http://doi:10.1016/j.matpr.2020.08.543

[30] Mishra, S., Prakash, A., Roy, S. K., Sharan, P., & Mathur, N. (2020). Breast Cancer Detection using Thermal Images and Deep Learning. 2020 7th International Conference on Computing for Sustainable Global Development (INDIACom). doi:10.23919/indiacom49435.2020.9083722

[31] Ibrahim, Abdelhameed; Mohammed, Shaimaa; Ali, Hesham Arafat and Hussein, Sherif E. (2020). Breast Cancer Segmentation from Thermal Images Based on Chaotic Salp Swarm Algorithm. IEEE Access, 1–1. http://doi:10.1109/ACCESS.2020.3007336

[32] Kakileti, Siva Teja; Manjunath, Geetha and Madhu, Himanshu J. (2019). 41st Annual International Conference of the IEEE Engineering in Medicine and Biology Society (EMBC) - Cascaded CNN for View Independent Breast Segmentation in Thermal Images. 6294–6297. http://doi:10.1109/embc.2019.8856628

[33] Husaini, Mohammed Abdulla Salim Al; Habaebi, Mohamed Hadi; Hameed, Shihab A.; Islam, Md. Rafiqul and Gunawan, Teddy Surya (2020). A Systematic Review of Breast Cancer Detection Using Thermography and Neural Networks. IEEE Access, 8, 208922–208937. http://doi:10.1109/ACCESS.2020.3038817

[34] Raghavendra, U; Gudigar, Anjan; Rao, Tejaswi N; Ciaccio, Edward J; Ng, E.Y.K. and Rajendra Acharya, U. (2019). Computer aided diagnosis for the identification of breast cancer using thermogram images: A

comprehensive review. Infrared Physics & Technology, 103041–. http://doi:10.1016/j.infrared.2019.103041

[35] Farooq, Muhammad Ali and Corcoran, Peter (2020). 31st Irish Signals and Systems Conference (ISSC) - Infrared Imaging for Human Thermography and Breast Tumor Classification using Thermal Images. 1–6. http://doi:10.1109/ISSC49989.2020.9180164

[36] Singh, Deepika and Singh, Ashutosh Kumar (2020). Role of image thermography in early breast cancer detection- Past, present and future. Computer Methods and Programs in Biomedicine, 183, 105074–. http://doi:10.1016/j.cmpb.2019.105074

[37] Kakileti, Siva Teja; Madhu, Himanshu J.; Manjunath, Geetha; Wee, Leonard; Dekker, Andre and Sampangi, Sudhakar (2020). Personalized risk prediction for breast cancer pre-screening using artificial intelligence and thermal radiomics. Artificial Intelligence in Medicine, 105, 101854–. http://doi:10.1016/j.artmed.2020.101854

[38] SÃ¡nchez-Ruiz, Daniel; Olmos-Pineda, Ivan and Olvera-LÃ³pez, J. Arturo (2020). Automatic region of interest segmentation for breast thermogram image classification. Pattern Recognition Letters, 135, 72–81. http://doi:10.1016/j.patrec.2020.03.025

[39] Mahmood, Tariq; Li, Jianqiang; Pei, Yan; Akhtar, Faheem; Imran, Azhar and Rehman, Khalil ur (2020). A Brief Survey on Breast Cancer Diagnostic with Deep Learning Schemes Using Multi-Image Modalities. IEEE Access, 1–1. http://doi:10.1109/ACCESS.2020.3021343

[40] P, Gomathi; C, Muniraj and PS, Periasamy (2020). BREAST THERMOGRAPHY BASED UNSUPERVISED ANISOTROPIC- FEATURE TRANSFORMATION METHOD FOR AUTOMATIC BREAST CANCER DETECTION. Microprocessors and Microsystems, 103137–. http://doi:10.1016/j.micpro.2020.103137

[41] DMR - Database for Mastology Research. Retrieved from http://visual.ic.uff.br/dmi/

[42] Y. LeCun, B. Boser, J. S. Denker, D. Henderson, R. E. Howard, W. Hubbard, and L. D. Jackel. Backpropagation applied to handwritten zip code recognition. Neural computation, 1(4):541–551, 1989.

[43] P. Sermanet, D. Eigen, X. Zhang, M. Mathieu, R. Fergus, and Y. LeCun. Overfeat: Integrated recognition, localization and detection using convolutional networks. arXiv:1312.6229, 2013.

[44] A. Krizhevsky, I. Sutskever, and G. E. Hinton. Imagenet classification with deep convolutional neural networks. In NIPS, 2012.

[45] K. Simonyan and A. Zisserman. Very deep convolutional networks for large-scale image recognition. In ICLR, 2015.

[46] M. Holschneider, R. Kronland-Martinet, J. Morlet, and P. Tchamitchian. A real-time algorithm for signal analysis with the help of the wavelet transform. In Wavelets: TimeFrequency Methods and Phase Space, pages 289–297. 1989.

[47] A. Giusti, D. Ciresan, J. Masci, L. Gambardella, and J. Schmidhuber. Fast image scanning with deep max-pooling convolutional neural networks. In ICIP, 2013.

[48] L.-C.Chen,G.Papandreou,I.Kokkinos,K.Murphy,andA.L. Yuille. Deeplab: Semantic image segmentation with deep convolutional nets, atrous convolution, and fully connected crfs. arXiv:1606.00915, 2016.

[49] A. Brandt. Multi-level adaptive solutions to boundary-value problems. Mathematics of computation, 31(138):333–390, 1977.

[50] D. Terzopoulos. Image analysis using multigrid relaxation methods. TPAMI, (2):129–139, 1986.

[51] K. Grauman and T. Darrell. The pyramid match kernel: Discriminativeclassificationwithsetsofimagefeatures. InICCV, 2005.

[52] S. Lazebnik, C. Schmid, and J. Ponce. Beyond bags of features: Spatialpyramidmatchingforrecognizingnaturalscene categories. In CVPR, 2006.

[53] W. Liu, A. Rabinovich, and A. C. Berg. Parsenet: Looking wider to see better. arXiv:1506.04579, 2015.

[54] S. Ioffe and C. Szegedy. Batch normalization: Accelerating deep network training by reducing internal covariate shift. arXiv:1502.03167, 2015.

[55] Chen, L.C., Papandreou, G., Schroff, F., Adam, H.: Rethinking atrous convolution for semantic image segmentation. arXiv:1706.05587 (2017)

[56] Ronneberger, O., Fischer, P., Brox, T.: U-net: Convolutional networks for biomedical image segmentation. In: MICCAI. (2015).

[57] Sandeep Wadekar, Dileep Kumar Singh. (2023). A modified convolutional neural network framework for categorizing lung cell histopathological image based on residual n. Elsevier. 4, pp.1-8. [Online]. Available at: https://doi.org/10.1016/j.health.2023.100224

[57] MYASAR MUNDHER ADNAN, MOHD SHAFRY MOHD RAHIM, AMJAD REHMAN KHAN. (2023). Automated Image Annotation with Novel Features Based on Deep ResNet50-SLT. IEEE. 11, pp.40258-40277. [Online]. Available at: Digital Object Identifier 10.1109/ACCESS.2023.3266296.

[58] Liu, Zhiyong; Yang, Chuan; Huang, Jun; Liu, Shaopeng; Zhuo, Yumin; Lu, Xu (2021). Deep learning framework based on integration of S-Mask R-CNN and Inception-v3 for ultrasound image-aided diagnosis of prostate cancer. Future Generation Computer Systems, 114, pp.358–367. doi:10.1016/j.future.2020.08.015